A Detailed Look into Power Consumption of Commodity 60 GHz Devices

Swetank Kumar Saha[1], Tariq Siddiqui[1], Dimitrios Koutsonikolas[1], Adrian Loch[2], Joerg Widmer[2], Ramalingam Sridhar[1]
[1]University at Buffalo, The State University of New York, [2]IMDEA Networks Institute, Spain, Madrid
Email: {swetankk,tariqsid,dimitrio,rsridhar}@buffalo.edu,{adrian.loch,joerg.widmer}@imdea.org

***Abstract*—The millimeter-wave technology is emerging as an alternative to legacy 2.4/5 GHz WiFi, offering multi-Gigabit throughput. While a lot of attention has been paid recently to analyzing the performance of the 60 GHz technology and adapting it for indoor WLAN usage, the power consumption aspect has largely been neglected. Given that mobile devices are the next target for 60 GHz, any discussion about this technology is incomplete without considering power consumption.**

In this work, we present the first, to our best knowledge, detailed study of the power consumption of 60 GHz commodity devices. We evaluate the power and energy consumption of two standard-compliant 60 GHz wireless adapters in different operating states and under a number of different configurations. We also compare our results against 802.11ac and discuss power-performance tradeoffs for the two technologies.

I. Introduction

We experience today an explosion in wireless network traffic driven by the rapidly growing number of mobile devices and bandwidth hungry applications. Industry predicts that the aggregate bandwidth demands will increase by 1000x by 2020 [1]. The use of millimeter-wave (mmWave) radios in the unlicensed 57-64 GHz spectrum (colloquially known as the 60 GHz band) has recently emerged as an alternative to the traditional WiFi and cellular systems, promising multi-Gbps rates. For example, the recently ratified 802.11ad standard [2] defines three 2.16 GHz channels and offers bitrates between 385 Mbps and 6.76 Gbps. More importantly, the order-of-magnitude shorter wavelengths in the 60 GHz band compared to the ISM band makes it possible to pack a very large number of antennas into small form factor antenna arrays. The small form factor combined with highly directional beams allows for very dense deployments and high spatial reuse.

Due to these characteristics, communication in the 60 GHz band has recently attracted significant interest in both industry and academia. 60 GHz technology is being seen as a strong candidate for building picocells in 5G cellular networks and recent measurement studies [3], [4] have demonstrated the feasibility of this approach. Another scenario of increasing interest is the use of the 60 GHz technology for building *multi-gigabit WLANs for indoor environments* [5], [6], [7]. These scenarios imply that battery-powered mobile devices will be the next target for mmWave technology. Recently, SiBeam announced the first 802.11ad equipped smartphone [8]. A study from ABI Research predicts that smartphones will account for nearly half of 802.11ad chipset shipments in 2018 [9].

A caveat is that improved communication speeds generally come at the cost of higher power consumption. Experimental studies with 802.11n/ac chipsets and smartphones over the past few years have shown that power increases with the PHY data rates [10], [11], [12] and channel width [13], [12], as well as with the application layer throughput [14], [15], [16], [17]. Although smartphones today typically come equipped with 802.11n/ac interfaces that support a 80 MHz channel width and 2x2 MIMO operation, popular 802.11n chipsets back in 2010 could deplete a smartphone's battery in under three hours and could emit nearly enough heat to burn a user's hand [10]. 802.11ad offers much higher data rates compared to 802.11ac (e.g., the minimum data rate is 6.5 Mbps for 802.11ac but 385 Mbps for 802.11ad) and an order of magnitude wider channels (20-160 MHz vs. 2.16 GHz), which can support much higher application layer throughputs. These three factors combined can result in significantly increased power consumption compared to 802.11ac interfaces. On the other hand, the first generation of commercial WiGig[1] [18] and 802.11ad devices use a simple single-carrier (SC), SISO PHY layer that is more power efficient compared to OFDM MIMO used in legacy 802.11n/ac devices; and the higher data rates in 60 GHz may result in lower *energy per bit* even if the total power consumption is higher. Hence, it becomes essential to understand the factors that affect the power consumption of the 60 GHz technology and the potential power-performance tradeoffs in comparison with legacy WiFi.

Additionally, due to the extremely small wavelength, signals in the 60 GHz band are easily blocked by obstacles such as walls, furniture, or humans, resulting in link outage. To overcome these challenges, 60 GHz radios are typically highly directional introducing new challenges, due to human blockage in dynamic environments and client mobility. 802.11ad uses a beam steering protocol that (i) aligns the Tx-Rx beam directions to maximize link SNR and recover from link outages due to mobility and (ii) tries to overcome link outages due to blockage by seeking alternative NLOS paths via reflections. Nonetheless, recent studies [5], [3], [6], [19] have shown that the overhead of this process may be prohibitively high, poten-

978-1-5386-2723-5/17$31.00

[1]WiGig was the predecessor of 802.11ad, merged into the 802.11ad amendment in 2012.

tially nullifying the benefits of electronically steerable antenna arrays. It is equally important to understand the potential impact of the beam steering process on power consumption.

In this work, we present the first, to our best knowledge, detailed study of the power consumption of 60 GHz NICs in commercial off-the-shelf devices. We conduct experiments with two different 60 GHz NICs: a device that supports the slightly dated WiGig standard and a newer generation device that conforms to the 802.11ad specification. We investigate the power consumption in various states of the wireless interface, the impact of a number of factors from different layers of the protocol stack on both throughput and power consumption, and the tradeoffs between these two metrics. We also compare our results against 802.11ac and discuss power-performance tradeoffs for the two technologies. Finally, we evaluate the power consumption of the beam-steering process.

The rest of the paper is organized as follows. Section II discusses the related work. Section III describes the devices we use in our study and our experimental methodology. Section IV discusses the power consumption of the three technologies considered in this paper – WiGig, 802.11ad, 802.11ac – in various non-communicating modes. Sections V-A and V-B examine the active (Tx/Rx) power and energy consumption of WiGig and 802.11ad and Section V-C compares the energy efficiency of 802.11ad against that of 802.11ac and discusses power-performance tradeoffs for the two technologies. Section VI compares the power consumption of the beam steering process in the WiGig and 802.11ad cards. Finally, Section VII concludes the paper.

II. Related work

A number of experimental works have studied the performance of commercial 60 GHz radios in outdoor picocell [3] and indoor data center [20], [21], [22] and WLAN environments [5], [6], [19], [23]. In contrast, the power consumption of the 60 GHz technology has not been given due attention. In our previous work [23], we conducted the first, to our best knowledge, preliminary study of 60 GHz power consumption using a WiGig interface in a laptop-dock link setup. We found that the idle power of WiGig is much higher compared to 802.11ac and the beam searching algorithm after a link outage also incurs a significant amount of power consumption, in addition to the performance penalty which was observed by previous studies. We also found that the WiGig receive (Rx) power consumption is much higher than its 802.11ac counterpart but the significantly higher data rates result in lower energy per bit.

This work differs from the one in [23] in the following ways: (i) We conduct experiments with two different radios. In addition to the WiGig radio in a laptop-dock link setup used in [23], we measure the power consumption of a newer, fully 802.11ad-compatible chipset in a typical WLAN setup, involving a laptop and a wireless router (instead of a dock). In fact, the majority of our experiments are conducted using this new setup. At the same time, the use of two different generations of chipsets allows us to compare the evolution of the technology in terms of power efficiency. (ii) In [23], we only measured the Rx power consumption. In this work, we provide a complete picture of the power consumption of the WiGig radio used in [23] by reporting results on the Tx power consumption. (iii) In [23], for our comparison with legacy WiFi, we only used calculations based on numbers reported in previous studies. In contrast, in this work, we measure the power consumption of an 802.11ac radio under different configurations (MCS, channel width, number of MIMO streams) and perform a *direct* comparison of the power consumption of the two technologies in the same environment.

III. Measurement methodology

A. Devices

We conducted measurements using two different 60 GHz off-the-shelf systems.

Our first setup (setup I) consists of a Dell Latitude E7440 laptop running Windows, equipped with a DW1601 chipset housing a Wilocity Wil6120 WiGig radio and a Dell Wireless Dock D5000. The dock also has a WiGig NIC and acts as an AP. The Wilocity radios are equipped with 2x8 phased array antennas with relatively wide main beams ($30^o - 40^o$) [22], [6] and support a subset of the single-carrier PHY data rates, from 385 Mbps to 3850 Mbps. Another laptop is connected to the dock through a Gigabit Ethernet NIC to generate/receive UDP traffic. The use of the Ethernet interface limits the throughput in our experiments to a theoretical bound of 1 Gbps. However, even under the best channel conditions the Tx throughput for the link was limited to 200 Mbps. Note that setup I represents the first-generation of commercial 60 GHz devices and is not fully 802.11ad compliant. For example, the laptop can receive and decode beacons from 802.11ad APs (e.g., our Netgear Nighthawk router used in setup II), but the association process fails.

Our second setup (setup II) is a Netgear Nighthawk® X10 Smart WiFi Router [24] and an Acer Travelmate P400M laptop. This setup was used for most of the experiments. The router has the QCA9008-SBD1 module housing the QCA9500 chipset from Qualcomm, supporting all the single-carrier 802.11ad data rates (up to 4.6 Gbps). The laptop carries the client-version of the module: QCA9008-TBD1, which houses 802.11ac, 802.11ad and BT chipsets. It runs a typical Linux OS (Fedora 24, kernel 4.x) and uses the open source wil6210 wireless driver to interface with the chipset. Both the router and the laptop use a 32-element phased antenna array on a separate chipset, connected to the main chipset using a MHF4 cable. A high-end desktop is connected to the router through a 10G LAN SFP+ interface to generate/receive UDP traffic. Although this setup should theoretically allow us to take advantage of multi-Gigabit speeds, we found that the maximum goodput (with MCS 12) is limited to around 2.3 Gbps.

In addition to the two 60 GHz systems, for comparison with legacy WiFi, we used a third setup (setup III) consisting of two desktops, each housing a WLE900N5-18 3x3 802.11ac adapter, featuring a QCA9880 v2 chipset and controlled by

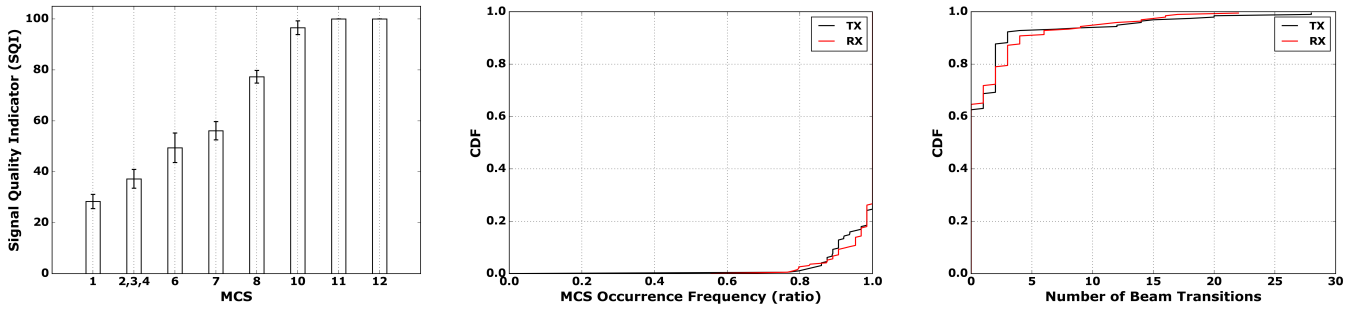

(a) SQI observed at each MCS during Tx measurements.

(b) Occurrence frequency of the desired MCS during each 10-sec measurement interval.

(c) Number of beam transitions on the client side during each 10-sec measurement interval.

Fig. 1. Stability of the channel quality and protocol parameters during the experiments.

the open source ath10k [25] driver. One is acting as a client and the other one as an AP (configured through hostapd).

B. Methodology

All our experiments were conducted in an academic office building at the University at Buffalo, which represents a typical scenario for future 802.11ad indoor WLANs. All experiments were performed late night to remove the possibility of human blockage. Unless otherwise stated, the experimental environment consisted of only static objects present in the building. Unless otherwise stated, each experiment consists of a 10-second backlogged UDP iperf/iperf3 session. All the results are the average of 5 sessions. We also plot the standard deviations as error bars.

The various 60 GHz radios used in setups I and II use their own rate adaptation algorithms and beamforming mechanisms to control beam properties. In case the link is blocked, the radios automatically search for an alternative NLOS path through a reflection to re-establish the connection. In setup I, we exported to the user-space the current *PHY data rate* and an *RSSI* value between 0 and 100 indicating received signal strength. In setup II, the wil6210 driver exports detailed connection parameters, including Tx and Rx MCS, beamforming (BF) status and sector in use, MAC layer goodput, and signal quality indicator (SQI). However, neither setup allows us to control the rate adaptation or beamforming mechanism, or to fix the MCS and BF sectors. Hence, in order to conduct measurements at different MCSs, we varied the link quality between the Tx and Rx either by changing the Tx-Rx distance or by introducing NLOS conditions. Although this methodology is not perfect, we note that the majority of our experiments were conducted under stable channel conditions, as shown in Figures 1(a), 1(b), 1(c).

Specifically, Figure 1(a) plots the average SQI value observed at each MCS, calculated over all the 10-sec Tx measurement intervals with a particular MCS (the graph for the Rx measurements is similar and omitted due to space limitations). We observe that the standard deviations are negligible for the highest MCSs and remain low for all MCSs except MCS 6, confirming that almost all measurements were taken under stable channel conditions. One concern is the fact the SQI values are low at low MCSs. Indeed, since we were not able to fix the MCS, the measurements for low MCSs were taken under poor link quality (e.g., long distances or NLOS conditions) that forced the rate adaptation algorithm to select the desired low MCS. This poor link quality may have an impact on the power consumption at low MCSs (due to an increased number of retransmissions), as we discuss in Section V-B. Figure 1(b) plots the cumulative distribution function (CDF) of the occurrence frequency of the desired MCS, separately for all the Tx and all the Rx measurements. The plots confirm that by varying the link conditions, we were able to force the rate adaptation algorithm to converge at the desired MCS in almost all the measurements. Specifically, the desired MCS was used exclusively in 75% of the 10-sec measurement intervals and at least 80% of the time in all 10-sec measurement intervals. Finally, Figure 1(c) plots the CDF of the number of beam transitions on the client side over all the Tx and Rx measurement intervals. We observe that in over 60% of the measurements, the selected beam never changed during the 10-sec interval and in 90% of the measurements the number of beam transitions was less than 5. Moreover, the long tail is due to MCS 1 measurements, which, as we mentioned above, were taken under poor link quality. If we exclude MCS 1, then the beam never changed in 65%/72% of the Tx/Rx measurements, and in 96%/100% of the Tx/Rx measurements the number of beam transitions was less than 4.

In contrast, setup III allows us to disable rate adaptation and statically configure MCS, channel width, and number of spatial streams for the 802.11ac radio. Hence, all our 802.11ac measurements were conducted under near-perfect channel conditions and we used a sniffer to ensure that there was no interference from other networks in the 5 GHz band.

C. Power Measurement

For setup I, we measured the power consumption of the wireless NIC, which comes in a Half-mini PCIE form factor, by plugging it to a PEX1-MINI-E PCI EXPRESS X1 to PCI Express Mini interface adapter [26]. This particular adapter allows us to power it from an external source and to take accurate measurements of power consumed by the NIC. Further, note that the client (Laptop) only exposes a Mini PCIE interface, so we used a Mini PCI-E to PCI-E Express X1 Riser

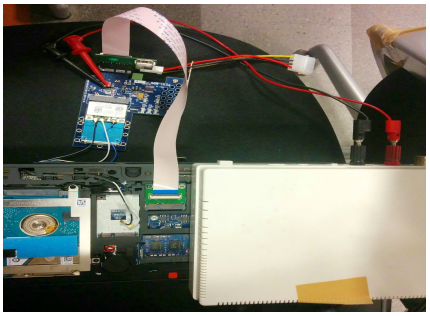

Fig. 2. Power measurement for setup I.

TABLE I
POWER IN NON-COMMUNICATING STATES (MW)

	WiGig	802.11ad	802.11ac
ON [Not Associated]	501	1058	282
SCAN	2729	1756	877
ON [Associated]	2351	1938	287
IDLE	2351	1938	955

Card along with a high speed extender cable to connect the adapter to the the laptop's Mini PCIE slot. Finally, we used a Monsoon Power Monitor [27] to supply power to the setup and record the power consumed. Figure 2 shows the complete setup.

For setup II, the methodology was similar but simpler. Originally, the chipset interfaces with the laptop using a M.2 (NGFF) slot. We removed the chipset from the laptop and used a M.2 E-keyed extender/adapter (M2-E3030-FLEX [28]). The extender connects to the laptop's M.2 port on one end and exposes a M.2 slot on the other end for plugging-in the 802.11ad chipset. Like in setup I, the extender allows for the chipset to be powered externally and power drawn to be measured.

The chipset used in setup III has a PCI-e based interface allowing us to use the same configuration as in setup I.

For all three setups, we also calculated the per-bit energy consumption (in nJ/bit) as the average power consumption (W=J/s) divided by the throughput/goodput (Mbps).

IV. POWER IN NON-COMMUNICATING STATES

We begin by examining the power in various non-communicating states. The results for the three setups (WiGig, 802.11ad, and 802.11ac) are shown in Table I. We distinguish four different states/modes, each of them described below.

ON [Not Associated] The *ON [Not Associated]* state is the lowest power setting for each of the three devices. Since we switched off auto-scanning and there was no Tx/Rx activity during these measurements, the reported power value indicates the minimum power that needs to be supplied to keep the card powered on. WiGig consumes almost half the power ($\sim$500 mW) compared to 802.11ad ($\sim$1000 mW) in this state. The 802.11ac chipset, however, requires only around 280 mW to stay up. Both the WiGig and 802.11ad wireless adapters actually host a legacy 2x2 802.11n and Bluetooth within the same module as the 802.11ad solution. Although we disabled both WiFi and Bluetooth interfaces, it is possible that some shared electronics cannot be turned off independently, resulting in higher power consumption compared to 802.11ac.

SCAN The scanning state consumes more than 2500 mW and 1700 mW for WiGig and 802.11ad devices, respectively. On the other hand, for the 802.11ac device, the scanning procedure consumes only around 900 mW. The significantly higher power consumption of the 60 GHz cards might be a concern for mobile devices. However, we found that the scan operation for the 802.11ad device is very efficient taking roughly 0.6 s, even shorter than the 802.11ac scanning time of roughly 1 s. Hence, the gap in the energy consumption between the two devices is much smaller than the power gap, 1.02 J (802.11ad) vs. 0.9 J (802.11ac). On the other hand, the scanning operation of the WiGig devices lasts considerably longer, around 3.5 s. The short scanning duration of the 802.11ad device was a surprise, since in the literature [3], [6] AP discovery in 60 GHz is considered as a challenging/time-taking task due to the directional beacon transmissions and the requirement for a full 360^o sweep. On the other hand, note that in 802.11ad only 3 channels have to be scanned in search of an AP, as opposed to more than 20 channels for 802.11ac. The much smaller number of channels combined with smart scanning/neighbor discovery algorithms suggest that scanning might not be a serious concern from either a performance or an energy aspect in future 60 GHz WLANs.

ON [Associated] In the *ON [Associated]* state (often referred to as base power), the devices are associated to the AP/Dock but there is no traffic sent to or received from the AP/Dock, except periodic beacons (or other control packets). This state is marked by much higher power consumption for both WiGig and 802.11ad cards. The WiGig radio consumes an additional 1849 mW of power when connected to the Dock, almost 4.6x the power drawn when it is disconnected. The 802.11ad device consumes additional 900 mW (1.8x the power of disconnected state) of power when connected to the Access Point. However, in contrast to the ON [Not Associated] state, 802.11ad's total power consumption in the ON [Associated] state is lower compared to WiGig by 413 mW. The 802.11ac power consumption remains at almost the same level as in the disconnected state, around 287 mW. This is due to Power Saving Mode (PSM), where the chip is put to sleep and only wakes up once every 100 ms to receive beacons. The total power consumption of WiGig/802.11ad in the ON [Associated] state is much higher than that of 802.11ac – 2.3[2]/1.9 W vs. 287 mW. In fact, it is higher than the Rx power and even comparable to the Tx power of certain 802.11ac configurations (Figures 7(b), 7(e)). The reason for this higher consumption is the much wider channel that needs to be correlated against for detecting incoming packets.

IDLE The *IDLE* state refers to the high-power state following a packet transmission/reception but before the chipset is put into low-power sleep or Power Saving Mode (PSM), after the expiry of the inactivity timer. For the 802.11ac chipset we used, the inactivity timer was 100 ms and the IDLE power consumption is equal to 955 mW. On the other hand, we

[2]We occasionally observed this value to vary between 3.5 - 4 W, e.g., just after re-connection. We believe that this is an energy bug in the chipset that leaves it in a high-power state after certain specific events.

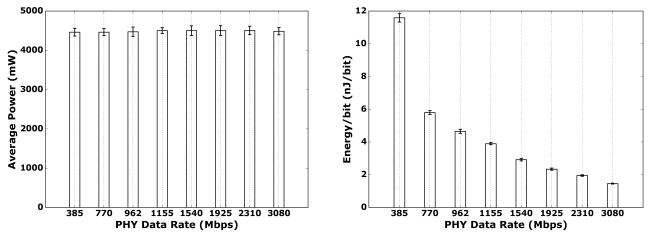

(a) Power consumption. (b) Energy per bit.

Fig. 3. Setup I: WiGig Tx power and energy per bit for different MCSs.

found that, in current WiGig/802.11ad devices, the power drops immediately to the ON [Associated] levels after a packet transmission/reception. This means that either (i) there is no inactivity timer in WiGig/802.11ad and the radio switches immediately to a (very power-hungry) sleep state of 2.3/1.9 W or (ii) there is no PSM implementation in WiGig/802.11ad and the radio is never put to sleep. In any case, the significantly high power consumption of the 60 GHz radio in the absence of any Tx/Rx activity (ON [Associated]) is a serious concern as smartphones become the next target of the 60 GHz technology.

V. Active Power Consumption

We now examine the active (Rx and Tx) power consumption of WiGig and 802.11ad in Sections V-A and V-B, respectively, and compare it against WiFi (802.11ac) in Section V-C.

A. Setup I: WiGig

We begin with the WiGig DW1601 chipset. Since this is a 1st generation chipset, not fully 802.11ad compatible, we only provide a brief discussion here (also, note that we studied its Rx power consumption in [23]). Our goal is to use this as a reference point in our detailed study of the 802.11ad power consumption in the next section and observe the evolution of the 60 GHz hardware in terms of power efficiency.

Figures 3(a), 3(b) plot the power consumption and energy per bit, respectively, as a function of the MCS with the WiGig DW1601 chipset in Tx mode. Since the Tx throughput with this radio is limited to only 200 Mbps (see Section III-A), the energy per bit values in Figure 3(b) are actually the *minimum* values obtained as the ratio of the measured power consumption over the corresponding PHY data rate. Figure 3(a) shows that Tx power consumption remains constant for all MCSs with an average value of 4.5 W and a standard deviation of 0.15-0.2 W. In [23], we found that the Rx power consumption for the same radio has the same mean value with a higher standard deviation (0.5 W). Hence, the radio has only two states when it is connected to the dock: *connected/idle* with a power consumption of 2.3 W (Table I) and *connected/active* with a power consumption of 4.5 W (96% higher). In contrast, legacy WiFi radios typically have two distinct active power states (Tx and Rx), with the Rx power consumption typically being lower. Figure 3(b) shows that the minimum energy per bit cost varies from 11.6 nJ/bit (for MCS 1) to as low as 1.75 nJ/bit (for MCS 12). Overall, the results here show that although the very high active power consumption (almost double compared to the already high idle power) is a concern for 60 GHz radios, the supported multi-gigabit PHY data rates have the potential to keep the per bit energy cost low, especially at high MCSs.

B. Setup II: 802.11ad

We now examine the 802.11ad active power consumption using the 802.11ad compliant QCA9500 chipset.

Impact of MCS Figures 4(a), 4(b), 4(c) plot the throughput, power consumption, and energy per bit, respectively as a function of the MCS with the 802.11ad QCA9500 chipset in Tx mode. Figures 4(d), 4(e), 4(f) plot the same metrics in Rx mode. Note that, in spite of numerous tests at multiple locations in both LOS and NLOS conditions, we never observed MCS 5 and MCS 9. Also, we were never able to find a location where MCS 2, 3 or 4 remained stable over a 10 sec period; the rate adaptation kept oscillating among these three data rates. Hence, in Figures 4(a)-4(f), we show one result for these three MCS indexes, denoted as "2,3,4".

In Figures 4(a), 4(d), we observe that the Tx and Rx throughputs in setup II (with the 2nd generation 802.11ad chipset) are symmetric, unlike in setup I (with the 1st generation WiGig chipset). Also, the maximum achievable throughput now exceeds 2 Mbps in both Tx and Rx mode (vs. 900 Mbps only in setup I). However, we still notice that throughput stops scaling with the MCS for MCS 10-12 due to hardware limitations, as we mentioned in Section III. Hence, to get a better idea of the achievable throughputs (and consequently the energy per bit) at higher MCS, we also plot the *Projected* throughput for MCS 10-12 in Tx mode and 11-12 in Rx mode using linear regression. We observe that even the projected values are far from the corresponding data rates; e.g., the maximum projected throughput ($\sim$2.5 Gbps) is only only 55% of the MCS 12 PHY data rate (4.6 Gbps). Given that the measurements for MCS 12 were taken under maximum SQI (Figure 1(a)), we conjecture that the reduced throughput is due to hardware limitations.

Figures 4(b), 4(e) show that MCS again has practically no impact on the power consumption, similar to what we observed in Section V-A with the WiGig chipset. However, we observe a drastic reduction in the total power consumption between the two generations of chipsets; the power consumption of the 802.11ad chipset is only 2-2.3W in both Tx and Rx mode, roughly half compared to the power of the WiGig chipset. Interestingly, the power consumption in Rx mode is slightly higher than in Tx mode for a given MCS. Also interestingly, the Tx power is slightly lower (100-200 mW) for higher MCSs. This could be the result of either power control running at the radio or an increased number of retransmissions and/or beam switches at lower MCSs under poor link quality, as we explained in Section III-B (Figures 1(a), 1(c)).

Figures 4(c), 4(f) show that the measured/projected energy per bit cost of the 2nd generation 802.11ad chipset is already lower than the minimum energy cost of the 1st generation WiGig chipset (Figures 3(b)), varying from 1-7.5 nJ/bit in Tx mode (vs. 1.75-11.6 nJ/bit for WiGig) and 1-9 nJ/bit in Rx mode. Additionally, the minimum energy per bit in

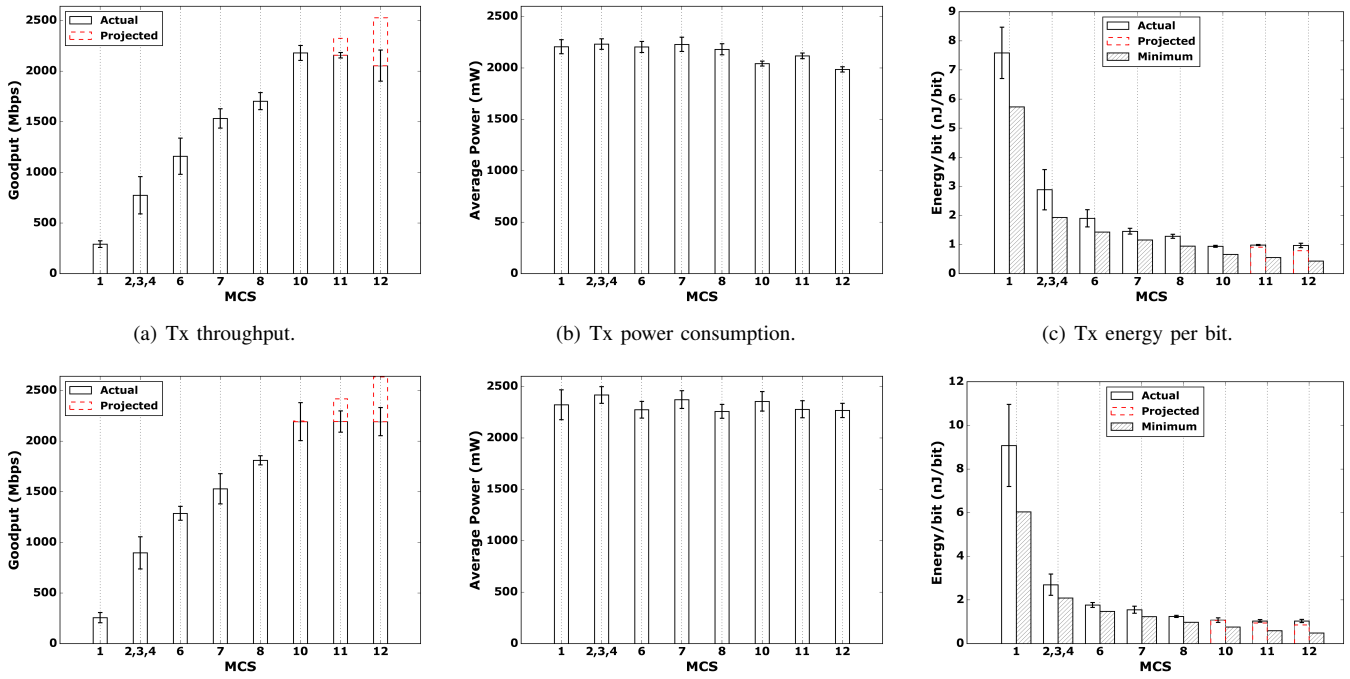

(a) Tx throughput. (b) Tx power consumption. (c) Tx energy per bit.

(d) Rx throughput. (e) Rx power consumption. (f) Rx energy per bit.

Fig. 4. Setup II: 802.11ad throughput, power, and energy per bit for different MCSs.

Figures 4(c), 4(f) varies between 0.5-5.8 nJ/bit in Tx mode and 0.5-6 nJ/bit in Rx mode, suggesting that there is still much room for further improvements in terms of power efficiency.

Impact of packet size Figures 5(a)/5(d) plot the Tx/Rx throughput, respectively, for different MCSs, as a function of the packet size. As expected, smaller packet sizes result in reduced throughput, especially for higher MCSs, due to higher MAC/PHY overhead. The impact is more pronounced in the case of Tx mode. For example, with MCS 12 and a 1000-byte packet size, the Tx throughput is 2.1 Gbps while the Rx throughput is only 1.25 Gbps.

Figures 5(b)/5(e), 5(c)/5(f) plot the Tx/Rx power and energy per bit, respectively, for different MCSs, as a function of the packet size. In [23], we found using setup I that the packet size has a small but non-negligible impact on the Rx power consumption. As it increases from 100 to 1400 bytes, the power consumption increases by 10%. Figure 5(e) shows a similar trend for setup II; the Rx power increases by 100-200 mW (5-10%) as the packet size increases from 100 to 1470 bytes. In contrast, we do not observe any clear trend for the Tx power consumption in Figure 5(b). From both these figures, we also observe that, for any given packet size, a higher MCS typically results in slightly lower power consumption (similar to the observation in Figure 5(a)). The large impact of small packet sizes on throughput combined with the small impact on power consumption result in a significant increase in the energy cost per bit in the case of small packet sizes, as shown in Figures 5(c), 5(f). The Tx energy per bit increases from 6 nJ/bit to 13 nJ/bit (116% increase) for MCS 1 and from 1-2 nJ/bit to 5.5-6 nJ/bit for other MCSs with 100-byte packets. The increase in the Rx energy per bit is smaller for MCS 1 (from 9 nJ/bit to 12 nJ/bit) but slightly larger in the case of other MCSs (from 1-2 nJ/bit to 7 nJ/bit).

Impact of source data rate While in all previous measurements we used backlogged traffic, we now evaluate the power consumption and energy per bit with different source rates, as in practice, applications might limit the sending data rate. In such cases, the radio remains idle between consecutive packet transmissions/receptions and the total power consumption is a weighted sum of the idle and active (Tx/Rx) power consumption. We plot the Tx/Rx power consumption and energy per bit, respectively for different MCSs, as a function of the source data rate in Figures 6(a)/6(c), 6(b)/6(d). We performed experiments with different sets of source rates for each MCS, making sure that all rates in a set targeting a particular MCS can be supported by that MCS.

Figures 6(a), 6(c) show an interesting trend of the power consumption as a function of the source data rate. Based on previous studies in legacy WiFi [15], [17], one would expect the power consumption to increase with the source data rate, as higher source rates keep the radio on for a larger fraction of time. In contrast, Figures 6(a), 6(c) show that the power drops by 100-200 mW for a source rate of 500 Mbps and then increases again; this behavior is persistent for all MCSs except MCS 1. While we cannot explain this behavior, we conjecture that it might be due to frame aggregation, as different source rates might result in different numbers of aggregated frames.

In the case of 802.11n/ac, previous measurement studies [10], [29], [12] have shown that the "race-to-sleep" heuristic, i.e., transmitting always at the highest possible PHY data rate, does not always work, especially for low source rates, as the energy savings from finishing the data transfer faster are

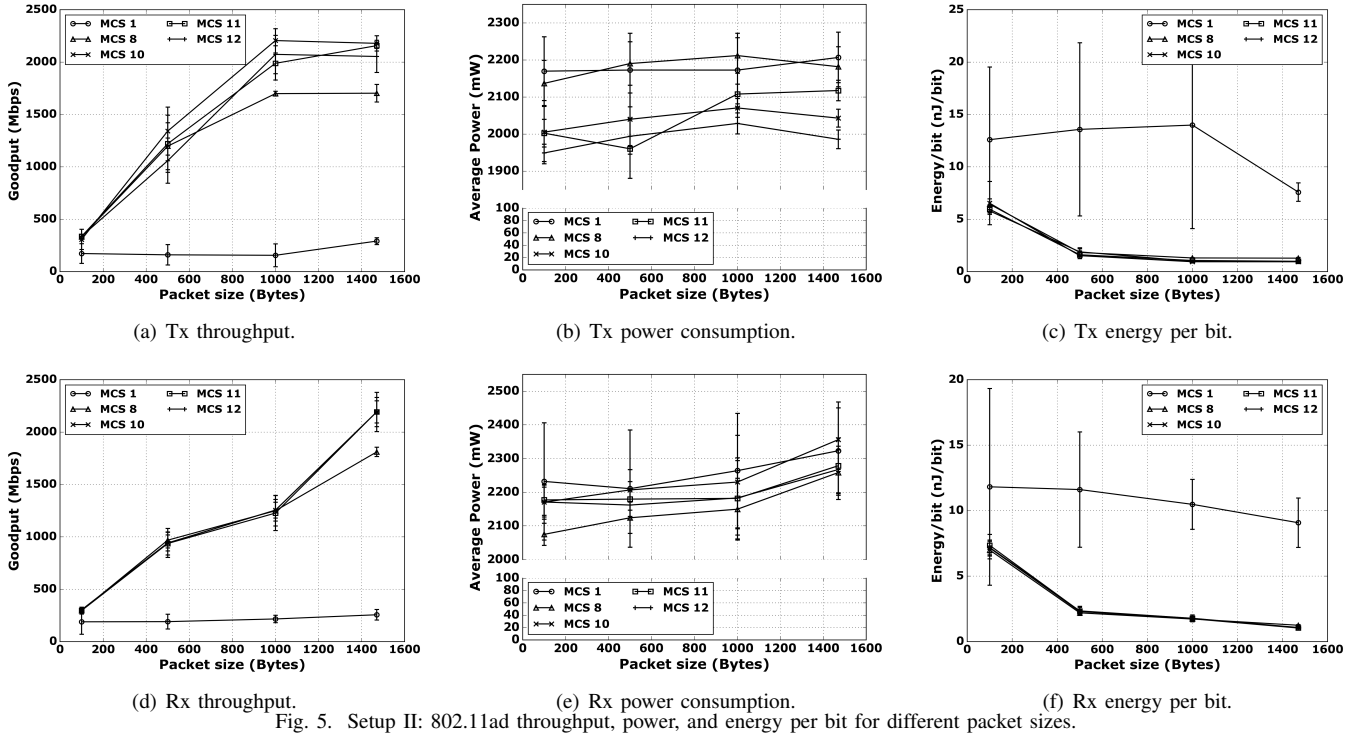

(a) Tx throughput. (b) Tx power consumption. (c) Tx energy per bit.

(d) Rx throughput. (e) Rx power consumption. (f) Rx energy per bit.

Fig. 5. Setup II: 802.11ad throughput, power, and energy per bit for different packet sizes.

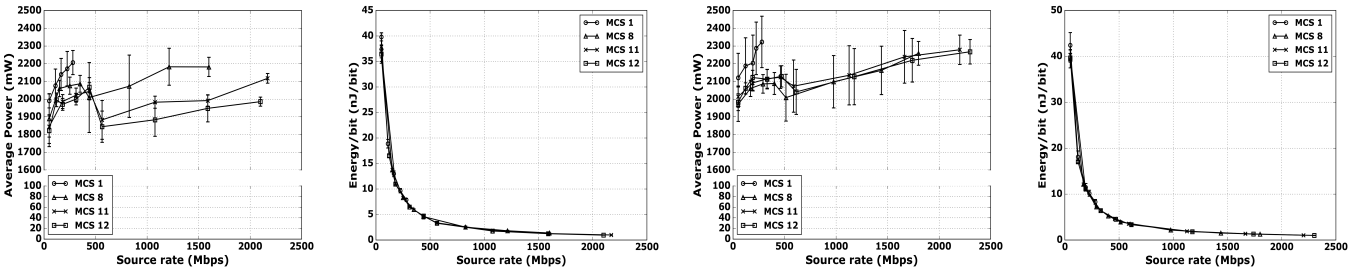

(a) Tx power consumption. (b) Tx energy per bit. (c) Rx power consumption. (d) Rx energy per bit.

Fig. 6. Setup II: 802.11ad power and energy per bit for different source data rates.

counter-balanced by the extra power consumed by higher order MCS, wider channels, or multiple MIMO streams, required to achieve a higher PHY data rates. In the case of 802.11ad, the channel width is fixed, the radio supports only one stream (SISO), and the power consumption is slightly lower for higher MCSs in Tx mode (Figure 6(a)). Accordingly, the "race-to-sleep" heuristic generally holds, i.e., the fastest MCS is the most energy efficient in Tx mode, as shown in Figures 6(b), although the difference between different MCSs is very small due to the small differences in power consumption. In Rx mode, the differences between different MCSs in terms of power consumption are even smaller and the energy per bit cost is almost identical for all MCSs except MCS1.

C. Comparison with 802.11ac

Finally, for comparison, we evaluate the power consumption of the QCA9880 802.11ac chipset in setup III. Note that, in contrast, to the single-carrier, single channel width, SISO 802.11ad PHY layer, 802.11ac supports an OFDM-based PHY layer, 3 different channel widths (20/40/80 MHz), and multiple MIMO spatial streams – up to 3 in our case denoted as SS (single stream), DS (double stream), and TS (triple stream). Also, unlike WiGig/802.11ad, where there is a one-to-one mapping between MCS and PHY data rate, in 802.11ac the PHY data rate is determined by the combination of MCS, channel width, number of spatial streams, and guard interval, and different combinations can result in the same data rate. In the following, we show results for different combinations of MCS, channel width, and number of spatial streams, but fix the guard interval at 400 ns.

Figures 7(a), 7(b), 7(c) plot the throughput, power consumption, and energy per bit, respectively, as a function of the PHY data rate with the 802.11ad QCA9500 chipset in Tx mode. Figures 7(d), 7(e), 7(f) plot the same metrics in Rx mode. For a fair comparison, we focus on configurations that can support PHY data rates commensurate to those supported by 802.11ad (i.e., at least 385 Mbps), and show the results only for those rates. For example, there is no SS configuration and 40MHz-DS has only a single point at 400 Mbps (MCS 9).

The comparison of Figures 7(a), 7(d) with Figures 4(a), 4(d)

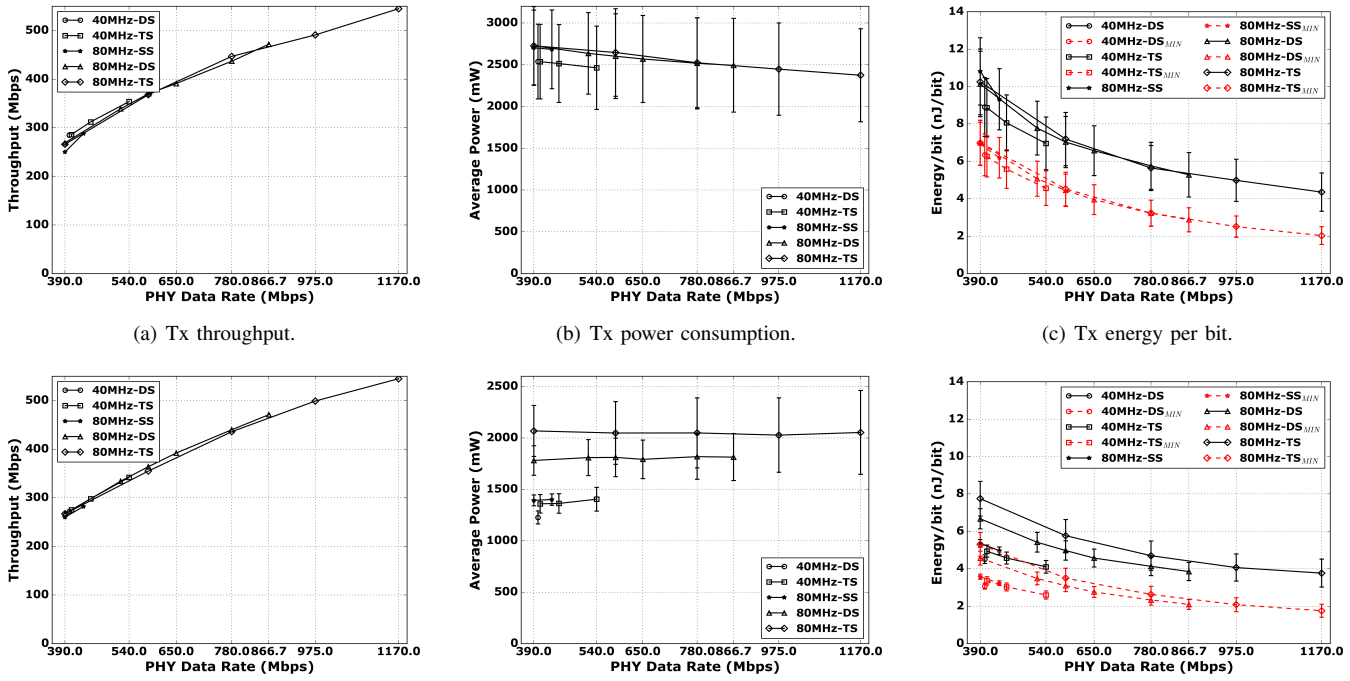

(a) Tx throughput. (b) Tx power consumption. (c) Tx energy per bit.

(d) Rx throughput. (e) Rx power consumption. (f) Rx energy per bit.

Fig. 7. Setup III: 802.11ac throughput, power, and energy per bit for different combinations of MCS, channel width, and number of streams.

clearly shows the throughput gains of the 60 GHz technology. Even highest-rate 802.11ac configuration possible with our chipset (80 MHz-TS, MCS 9; data rate:1170 Mbps) can give a throughput of only 550 Mbps, roughly 25% of the maximum achievable throughput with 802.11ad (2 Gbps in Setup II).

Figures 7(b), 7(e) show that different combinations of channel width and number of spatial streams result in different levels of power consumption. We also observe that in contrast to 60 GHz radio, the 802.11ac power consumption is different in Tx and Rx mode. In Tx mode (Figure 7(b)), we observe that the dominant factor is the channel width, while the impact of the number of streams is negligible. We also clearly observe a small but non-negligible drop with the MCS. In Rx mode (Figure 7(e)), both the channel width and the number of spatial streams affect the power consumption but MCS has no impact.

More importantly, the comparison against 802.11ad (Figures 4(b), 4(e)) reveals that *the 802.11ac power consumption is often comparable to or even higher than the 802.11ad power consumption* in the case of backlogged traffic. Specifically, in Tx mode, the 802.11ac average power consumption varies from 2.45-2.55 W with a 40 MHz channel width and from 2.4-2.7 W with an 80 MHz channel width, i.e., it is always higher than the 802.11ad power consumption (2-2.3 W) for similar PHY data rates. In Rx mode, the 802.11ac power consumption with a 40 MHz channel width is quite lower compared to 802.11ad. The same is true for with 80MHz-SS/DS (below 1.5/1.8 W vs. 2.3 W) but it becomes similar (2.1 W) with 80MHz-TS.

Since 802.11ac can control the power consumption for a given target throughput via different channel width/spatial stream combinations, unlike 802.11ad, we divide the x-axis in Figures 7(c), 7(f) in two regions to study the per bit energy cost: PHY data rates lower than or equal to 540 Mbps, achievable by all 5 configurations in Figures 7(c), 7(f) and PHY data rates higher than 540 Mbps, achievable only by 80 MHz and DS/TS. We also consider only MCS 1-4 in 802.11ad (Figures 4(c), 4(f)), which achieve similar data rates (385-1155 Mbps).[3] In the first region, $[390Mbps, 540Mbps]$, 40 MHz configurations are the most energy efficient. Their energy cost is higher than that of 802.11ad in Tx mode (7-9 nJ/bit vs. 2.8-7.5 nJ/bit) but lower in Rx mode (4-5 nJ/bit vs. 2.8-7.5 nJ/bit). The same is true for the theoretically minimum energy costs. On the other hand, in the second region, where only 80MHz-DS/TS are possible, 802.11ad is more energy efficient than 802.11ac in both Tx mode (2.9 nJ/bit vs. 4.4-7 nJ/bit measured energy, 2 nJ/bit vs. 2-4.4 nJ/bit minimum energy) and Rx mode (2.8 nJ/bin vs. 3.9-5 nJ/bit measured energy, 2 nJ/bit vs. 1.9-3 nJ/bit minimum energy).

In Figures 8(a), 8(b) we perform a more direct comparison of the energy per bit between the two technologies by considering the most energy efficient configuration for each technology that can support a given source data rate. In the case of 802.11ad, all MCSs have similar per bit energy cost (Figures 6(b)/6(d)) and we always use MCS 12 in our comparison. For 802.11ac, we use Figures 7(e), 7(f) to select the most energy efficient configuration among the 5 ones shown in those figures that can support a given source rate. Since we consider source rates as low as 50 Mbps in Figures 8(a), 8(b), we note that for some of those rates, there might be more energy efficient 802.11ac configurations available (e.g., 20 MHz, or

[3]We acknowledge that this comparison is not perfect due to the fact that we were not able to take separate measurements for MCS 2, 3, and 4 in 802.11ad.

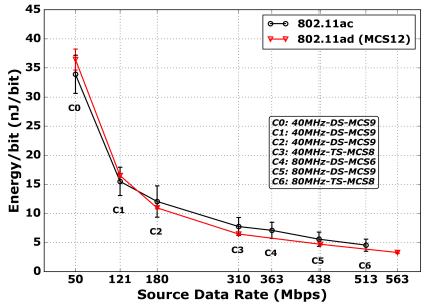

(a) Tx energy per bit.

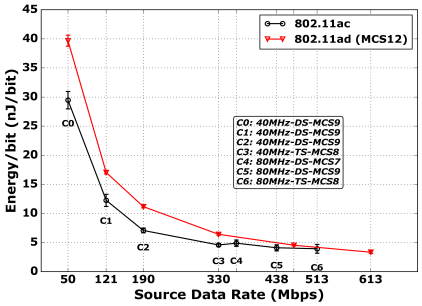

(b) Rx energy per bit.

Fig. 8. Comparison of the most energy efficient 802.11ad and 802.11ac configurations.

40MHz-SS). But, for a fair comparison between the two technologies, we only consider the 5 802.11ac configurations from 7(e), 7(f) having PHY data rates higher than 385 Mbps.

Figure 8(a) shows that 802.11ad has slightly higher Tx energy cost than 802.11ac for low source rates but becomes slightly more energy efficient at higher source rates, when 802.11ac has to activate TS or 80 MHz to support them. On the other hand, Figure 8(b) shows that 802.11ac is clearly more energy efficient in Rx mode, especially at low source rates (e.g., the gap is 10 nJ/bit at 50 Mbps), but the difference reduces reduces at higher source rates and becomes negligible after 400 Mbps. The cause behind the different energy efficiency of the two technologies under low vs. high source rates lies in the large disparity in their IDLE power, as we saw in Table I. Under low source rates, the radio spends more time in the IDLE state, which is much more power efficient for 802.11ac (955 mW) than for 802.11ad (1938 mW). In contrast, under high source rates, the radio stays on most of the time. In those cases, the 802.11ac power is comparable to or even higher (in Tx mode) than the 802.11ad power (Figures 4(b), 4(e) vs. Figure 7(b), 7(e)), especially with 80 MHz and 3 streams, resulting in lower per bit energy cost for 802.11ad.

Remarks: One parameter we have not considered in this study is the different range of the two technologies. Since the free space path loss is ∼22 dB higher in 60 GHz than in 5 GHz due to the smaller carrier wavelength, one can argue that 802.11ac achieves a better power-range tradeoff, as 802.11ad throughput will drop to 0 beyond a certain range, resulting in ∞ energy/bit. On the other hand, longer range comes at the cost of significantly reduced throughput. Indeed, the most robust 802.11ac configuration (MCS 0, 20 MHz, SS) yields a 2 orders of magnitude lower data rate than the lowest 802.11ad data rate (6.5 Mbps vs. 385 Mbps). Also, the high rate 802.11ac configurations (MCS 8/9, 80 MHz, TS) work only under very short ranges (in our setup, MCS 9, 80MHz-TS always resulted in zero throughput) while 802.11ad can sustain Gbps data rates up to 100-150 ft in typical indoor WLAN environments [23]. A detailed study of the power-performance-range tradeoffs between the two technologies is part of our future work.

VI. Beam Steering Power Consumption

The need for directional links in 60 GHz communication requires that devices perform a *beamforming* process before data transmission can take place and every time after a link breaks (due to blockage or mobility). This process enables the Tx and Rx ends of a link to discover the optimal beam to be used for data transmission. At the very least, it involves exchange of sounding/control packets through the different beam configurations available. Previous studies [5], [3], [6] have reported that this process can have a severe negative impact on performance. In this section, we take a look at the power cost of the beam searching process triggered by a temporary link outage.

WiGig Figure 9(a) shows that after disconnection (at 2 s), the beamforming process starts and lasts for around 3.5 s. The power in the region shows large variations between 1500-3600 mW. Moreover, another distinct power state follows the beamforming phase (marked as Re-Association) that lasts for 9-10 s, during which power remains almost constant (3600 mW) before dropping down back to the idle level (2000 mW). In different runs of this setup, the average power consumption of the beamforming phase varied from 2942-3344 mW and the combined power consumption of the Beamforming/Re-Association phase varied from 3406-3838 mW.

802.11ad Figure 9(b) shows the different power states that occur while the client tries to re-establish a working link with the AP. We mark the different power states in Figure 9(b) and also mention the Beamforming (BF) status as reported by the driver. Link blockage is introduced around the 9th second. As a first response, the driver attempts to recover the damaged link by trying alternate beams or trying to re-train the same beam again (region marked: "BF Status: Retrying"). The *retrying* phase lasts for about 2.24 s and consumes an average power of 1890.33 mW. Just after this period, the link is reported lost/broken and the chipset starts searching for the AP from scratch. In this particular scenario, it took the chip around 8.42 seconds, marked as disconnected in the figure, to re-establish the link. During this time period, there are three high-power periods with an average power of 1738.84 mW around the 13th, 19th and 21st seconds interleaved with lower-power periods (∼1315.28 mW). We verified, through a separate experiment, that those high-powered periods actually have a similar power-profile as channel scans. It is possible that the chipset performs repeated scans to look for beacons from the AP it was last connected to. Around the 22nd second the link is re-established and power consumption returns to same level as before the link blockage event.

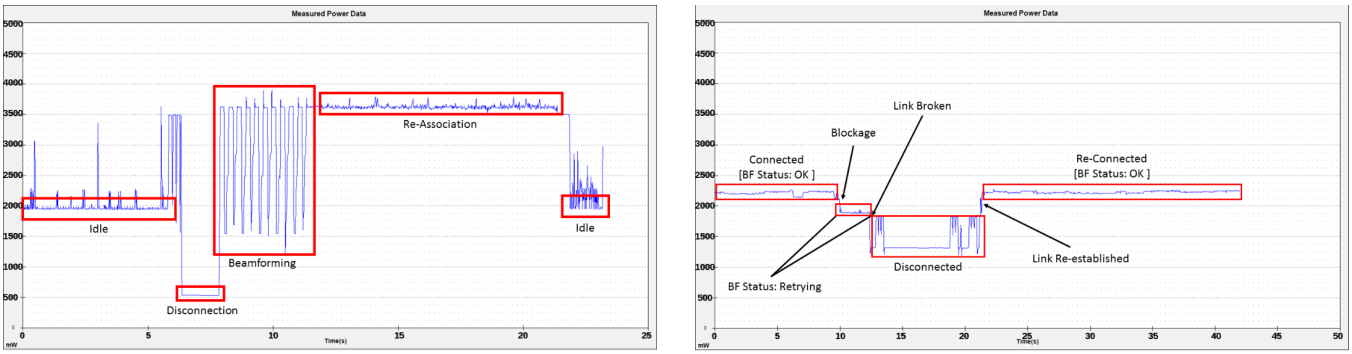

(a) WiGig (figure reproduced from [23]).

(b) 802.11ad.

Fig. 9. Power consumption in the case of temporary link outage and re-connection.

In summary, the newer generation 802.11ad devices appear to have improved the beam re-training process significantly both in terms of power consumption and duration, resulting in overall lower energy consumption. Where the WiGig device takes around 15 seconds with power levels close to 3.5 W to re-establish the link, the 802.11ad device does it within 10 seconds and consumes an average power of 1655.84 mW only. Nonetheless, beam-forming still has a considerable negative impact on power consumption and performance. There lies further need for more efficient beam searching algorithms.

VII. Conclusion

In this work, we presented what we believe to be the first detailed measurements of power consumption of commercial 60 GHz devices. We observed that the newer generation 802.11ad chipset is much more energy-efficient compared to its WiGig counterpart, due to its lower Tx/Rx power. However, 802.11ad's base power consumption of around 2.3W (compared to 802.11ac's 287 mW) is a cause for concern. Traffic mix on a real device is likely to be bursty, and a chipset could spend considerable amount of time in this state. We also compared the energy efficiency of 60 GHz devices with legacy WiFi (802.11ac) under different source data rates. At higher source rates approaching backlog, 802.11ad is more energy-efficient than 802.11ac as far as Tx is concerned. However, for Rx, 802.11ad always consumes more energy compared to 802.11ac. Lastly, we observed that, although the beamforming power consumption has decreased in the newer generation 802.11ad device, the beamforming process still incurs a significant power cost.

VIII. Acknowledgment

This work was supported in part by NSF grants CNS-1553447 and CNS-1422304, the European Research Council grant ERC CoG 617721, the Ramon y Cajal grant from the Spanish Ministry of Economy and Competitiveness RYC-2012-10788, and the Madrid Regional Government through the TIGRE5-CM program (S2013/ICE-2919).

References

[1] "Mobile broadband usage is set to explode," http://www.techjournal.org/2011/09/mobile-broadband-useage-is-set-toexplode-infographic.

[2] "IEEE 802.11 Task Group AD," http://www.ieee802.org/11/Reports/tgad_update.htm.

[3] Y. Zhu, Z. Zhang, Z. Marzi, C. Nelson, U. Madhow, B. Y. Zhao, and H. Zheng, "Demystifying 60ghz outdoor picocells," in *Proc of ACM MobiCom*, 2014.

[4] T. S. Rappaport, S. Sun, R. Mayzus, H. Zhao, Y. Azar, K. Wang, G. N. Wong, J. K. Schulz, M. Samimi, and F. Gutierrez, "Millimeter Wave Mobile Communications for 5G Cellular: It Will Work!" *IEEE Access*, vol. 1, May 2013.

[5] X. Tie, K. Ramachandran, and R. Mahindra, "On 60 GHz wireless link performance in indoor environments," in *Proc of PAM*, 2012.

[6] S. Sur, V. Venkateswaran, X. Zhang, and P. Ramanathan, "60 GHz Indoor Networking through Flexible Beams: A Link-Level Profiling," in *Proc. of ACM SIGMETRICS*, 2015.

[7] S. K. Saha, V. V. Vira, A. Garg, and D. Koutsonikolas, "60 GHz Multi-Gigabit Indoor WLANs: Dream or Reality?" *ArXiv e-prints*, September 2015.

[8] "SiBEAM Captures World's First 60GHz Millimeter-Wave Smartphone Design Win in Letv's Flagship Smartphone, Le Max," http://www.businesswire.com/news/home/20150519005350/en/SiBEAM-Captures-World's-60GHz-Millimeter-Wave-Smartphone-Design#.VZM9AkT9q9s.

[9] "Smartphones will Account for Nearly Half of Both 802.11ac and 802.11ad Chipset Shipments in 2018," https://www.abiresearch.com/press/smartphones-will-account-for-nearly-half-of-both-8, June 2013.

[10] D. Halperin, B. Greenstein, A. Sheth, and D. Wetherall, "Demystifying 802.11n power consumption," in *Proc. of USENIX Workshop on Power Aware Computing and Systems*, October 2010.

[11] N. Warty, R. K. Sheshadri, W. Zheng, and D. Koutsonikolas, "A first look at 802.11n power consumption in smartphones," in *Proc. of ACM PINGEN*, 2012.

[12] S. K. Saha, P. Deshpande, P. P. Inamdar, R. K. Sheshadri, and D. Koutsonikolas, "Power-throughput tradeoffs of 802.11n/ac in smartphones," in *Proc. of IEEE INFOCOM*, 2015.

[13] P. M. Yunze Zeng, Parth H. Pathak, "A First Look at 802.11ac in Action: Energy Efficiency and Interference Characterization," in *Proc. of IFIP Networking*, 2014.

[14] J. Huang, F. Qian, A. Gerber, Z. M. Mao, S. Sen, and O. Spatscheck, "A Close Examination of Performance and Power Characteristics of 4G LTE Networks," in *Proc. of ACM Mobisys*, 2012.

[15] P. Serrano, A. Garcia-Saavedra, A. Banchs, G. Bianchi, and A. Azcorra, "Per-frame energy consumption anatomy of 802.11 devices and its implication on modeling and design," *IEEE/ACM Transactions on Networking (ToN)*, vol. 23, no. 4, pp. 1243–1256, 2014.

[16] L. Sun, R. K. Sheshadri, W. Zheng, and D. Koutsonikolas, "Modeling WiFi Active Energy Consumption in Smartphones for App Developers," in *IEEE ICDCS*, 2014.

[17] S. K. Saha, P. Malik, S. Dharmeswaran, and D. Koutsonikolas, "Revisiting 802.11 Power Consumption Modeling in Smartphones," in *Proc. of IEEE WoWMoM*, 2016.

[18] C. Hansen, "WiGiG: Multi-gigabit wireless communications in the 60 GHz band," *IEEE Wireless Communications Magazine*, vol. 18, no. 6, December 2011.

[19] T. Nitsche, G. Bielsa, I. Tejado, A. Loch, and J. Widmer, "Boon and Bane of 60 GHz Networks: Practical Insights into Beamforming, Interference, and Frame Level Operation," in *Proc. of the 11th ACM CoNEXT*, December 2015.

[20] D. Halperin, W. Hu, A. Sheth, and D. Wetherall, "Predictable 802.11 packet delivery from wireless channel measurements," in *Proc. of ACM SIGCOMM*, 2010.

[21] X. Zhou, Z. Zhang, Y. Zhu, Y. Li, S. Kumar, A. Vahdat, B. Y. Zhao, and H. Zheng, "Mirror Mirror on the Ceiling: Flexible Wireless Links for Data Centers," in *Proc. of ACM SIGCOMM*, 2012.

[22] Y. Zhu, X. Zhou, Z. Zhang, L. Zhou, A. Vahdat, B. Y. Zhao, and H. Zheng, "Cutting the Cord: a Robust Wireless Facilities Network for Data Centers," in *Proc. of ACM MobiCom*, 2014.

[23] S. K. Saha, V. V. Vira, A. Garg, and D. Koutsonikolas, "A Feasibility Study of 60 GHz Indoor WLANs," in *Proc. of IEEE ICCCN*, 2016.

[24] "Netgear Nighthawk® X10." https://www.netgear.com/landings/ad7200.

[25] "ath10k: mac80211 wireless driver for qualcom atheros qca988x family of chips," http://wireless.kernel.org/en/users/Drivers/ath10k.

[26] "PCI EXPRESS X1 to PCI Express Mini interface adapter," http://www.adexelec.com/pciexp.htm.

[27] "Monsoon power monitor." http://www.msoon.com/LabEquipment/PowerMonitor/.

[28] "M2-E3030-FLEX." http://www.adexelec.com/m2.htm.

[29] C.-Y. Li, C. Peng, S. Lu, and X. Wang, "Energy-based rate adaptation for 802.11n," in *Proc. of the 18th Annual International Conference on Mobile Computing and Networking (MobiCom)*, August 2012.